Dielectric Relaxation of Dipole-Inverted *cis*-Polyisoprene Solutions

Hiroshi Watanabe,*,† Hirofumi Yamada,‡,§ and Osamu Urakawa‡,||

Institute for Chemical Research, Kyoto University, Uji, Kyoto 611, Japan, and Department of Macromolecular Science, Faculty of Science, Osaka University, Toyonaka, Osaka 560, Japan

Received April 6, 1995; Revised Manuscript Received June 26, 1995®

ABSTRACT: Dielectric relaxation behavior was examined for solutions of a series of *cis*-polyisoprene (PI) chains having almost identical molecular weights ($M \cong 48$K) but differently inverted type-A dipoles parallel along the chain contour. The solvent used was a dielectrically inert butadiene oligomer of $M = 0.7$K that was a moderately good solvent for the PI chains. Global motion of the dipole-inverted PI chains induced prominent dielectric relaxation at low frequencies, and the dielectric loss (ϵ'') curves changed their shape (frequency dependence) with increasing PI concentration c_{PI}: At c_{PI} smaller than the overlapping threshold c^* the ϵ'' curves were rather sharp and reasonably close to the prediction of the Tschoegl model considering both hydrodynamic and excluded-volume interactions, while for $c_{PI} > c^*$ the distribution became considerably broader than that predicted from the Rouse/Zimm/Tschoegl and reptation models. These dielectric changes were quite similar to those found in previous studies for PI solutions in Isopar-G and heptane. The shape of the ϵ'' curves reflected distribution of both relaxation times and intensities of dielectric modes, while those times and intensities were separately determined by characteristic times τ_p and integrated eigenfunctions $F_p(n)$ for eigenmodes of a local correlation function, $C(n,t;m) = \langle \mathbf{u}(n,t)\cdot\mathbf{u}(m,0)\rangle/\langle \mathbf{u}^2\rangle$, with $\mathbf{u}(n,t)$ being the nth bond vector at time t. For detailed examination of the above dielectric changes with c_{PI}, the ϵ'' data of the dipole-inverted PI chains were analyzed to evaluate $F_p(n)$ and τ_p (for the eigenmode index $p = 1-3$). At $c_{PI} \le c^*$, τ_p were almost proportional to $p^{-1.65}$ and $F_p(n)$ were nearly sinusoidal with respect to the segment location n. These results were in reasonable agreement with the Tschoegl model. With increasing $c_{PI} > c^*$, τ_p became almost proportional to p^{-2} while $F_p(n)$ became nonsinusoidal. This p dependence of τ_p was still in close agreement with the Rouse and/or reptation models, but the n dependence of $F_p(n)$ was considerably different. This result indicated that the broadening of the ϵ'' curves with c_{PI} was essentially due to changes in the eigenfunctions, not due to changes in the p dependence of τ_p (relaxation time span). Changes of $F_p(n)$ with c_{PI} were discussed in relation to coupling of motion of chains being overlapped at $c_{PI} > c^*$.

I. Introduction

cis-Polyisoprene (PI) chains have so-called type-A dipoles[1,2] parallel along their contour,[3] and their global motion induces slow, molecular weight (M) dependent dielectric relaxation. Utilizing this feature, extensive dielectric studies have been made for dynamics of PI chains in bulk,[3,5-8,14] blends,[7,9,10,15] and solutions.[4,7,11-13] A quantity describing fundamental aspects of the dielectric relaxation of the PI chains is a local correlation function,[14,15]

$$C(n,t;m) = (1/a^2)\langle \mathbf{u}(n,t)\cdot\mathbf{u}(m,0)\rangle \tag{1}$$

with $\mathbf{u}(n,t)$ being a bond vector for the nth segment at time t and $a^2 = \langle \mathbf{u}^2\rangle$. This function represents orientational correlation of segments at two separate times. At long time scales of global relaxation, $C(n,t;m)$ is written as a sum of its eigenmodes,[14]

$$C(n,t;m) = \frac{2}{N}\sum_{p=1}^{N} f_p(n)\, f_p(m)\, \exp(-t/\tau_p) \tag{2}$$

where f_p and τ_p are the eigenfunction and relaxation time for the pth eigenmode, and N is the number of segments of the chain. Characteristics of the chain dynamics are sensitively reflected in the p dependence of τ_p as well as in the functional form of $f_p(n)$, or equivalently in the form of integrated eigenfunctions defined by

$$F_p(n^*) = \frac{\sqrt{2}}{N}\int_0^{n^*} f_p(n)\, dn \tag{3}$$

F_p (or f_p) and τ_p are involved in dielectric quantities of type-A chains. For example, for *regular* PI chains having type-A dipoles aligned in the *same* direction from one end to the other, dielectric relaxation detects end-to-end vector fluctuation. For this case, dielectric loss (ϵ'') is written as[14]

$$\epsilon''(\omega) = \sum_{p=1}^{N} g_p \frac{\omega\tau_p}{1+\omega^2\tau_p^2} \tag{4}$$

with

$$g_p = 2\Delta\epsilon\left[\frac{1}{N}\int_0^N f_p(n)\, dn\right]^2 = \Delta\epsilon[F_p(N)]^2 \quad \text{(for regular PI chains)} \tag{5}$$

Here, $\Delta\epsilon$ is the total dielectric intensity for the global relaxation. As seen from eqs 4 and 5, the relaxation time of the pth dielectric mode is identical to τ_p for the pth eigenmode of C, while the pth dielectric intensity g_p is determined by the pth eigenfunction, F_p. Thus, changes in τ_p and F_p (or f_p) with various factors such as concentration and molecular weight are separately

* To whom correspondence should be addressed.
† Kyoto University (previously at Osaka University).
‡ Osaka University.
§ Current address: Department of Materials Science, Japan Advanced Institute of Science and Technology, Hokuriku, Nomi, Ishikawa 923-12, Japan.
|| Current address: Department of Polymer Science and Engineering, Kyoto Institute of Technology, Matsugasaki, Sakyo-ku, Kyoto 606, Japan.
® Abstract published in *Advance ACS Abstracts,* August 1, 1995.

0024-9297/95/2228-6443$09.00/0

reflected in changes in the relaxation times and intensities of the dielectric modes.

We here focus our attention on the effects of the PI concentration c_{PI} on dielectric behavior. Patel and Takahashi[11] and Urakawa et al.[12,13] studied dielectric relaxation of regular PI chains (without type-A dipole inversion) in solutions and found the following changes: In a dilute regime, the shape (frequency dependence) of ϵ'' curves is insensitive to c_{PI} and close to the prediction of the Rouse/Zimm model. With increasing c_{PI} in a semidilute regime, broadening of the ϵ'' curves takes place. Finally, in a concentrated regime the shape of the ϵ'' curves (broader than that in the dilute regime) again becomes independent of c_{PI}. These results indicate that the dielectric mode distribution is broadened with increasing c_{PI}. This broadening is certainly attributed to changes in the chain dynamics that could have affected both τ_p and F_p. However, the ϵ'' data for regular PI chains are not sufficient to further specify details of the changes in τ_p and F_p: As seen from eq 4, the shape of the ϵ'' curves is determined by two factors, relaxation time span (τ_p/τ_1 ratio) and dielectric intensity distribution (g_p/g_1 ratio) for the eigenmodes. The data for the regular PI chains do not clearly tell us whether the observed broadening of the ϵ'' curves corresponds to changes in the τ_p/τ_1 ratio or in the g_p/g_1 ratio, or both. In addition, for the regular PI chains g_p is related to F_p at a particular n value, $n = N$ (eq 5), so that the functional form of $F_p(n)$ reflecting the characteristics of chain dynamics cannot be specified even if we know the g_p values. Thus, details of the concentration dependence of τ_p and F_p were left unclear, although arguments[11-13,16] were made for the longest relaxation time τ_1 as well as for the dielectric mode distribution on the basis of the theories of Muthukumar–Freed[17] and Muthukumar.[18]

A breakthrough for the above problem is found from dielectric studies on PI chains having *inversion* of type-A dipoles at particular segments.[6,14,15] For a series of such PI chains having the same M but differently inverted type-A dipoles, the molecular motion is the same but the dielectric responses are quite different. As demonstrated in our previous papers,[14,15] this difference enables us to experimentally evaluate τ_p and $F_p(n)$. Considering this unique feature of the dipole-inverted PI chains, we examined their dielectric behavior in a moderately good solvent, a butadiene oligomer of $M = 0.7$K. We evaluated the τ_p and F_p for the lowest three eigenmodes ($p = 1-3$) from the ϵ'' data for those PI chains at various c_{PI}, examined the c_{PI} dependence of τ_p and F_p, and discussed details of changes in the dielectric mode distribution with c_{PI}. This paper presents the results.

II. Theoretical Section

A theoretical background for dielectric relaxation of dipole-inverted type-A chains and details of procedures for evaluation of F_p were described in our previous paper.[14] This section presents a brief summary.

For a type-A chain being composed of N segments and having dipole inversion at the n^*th segment, the total dipole $\mathbf{P}$ is proportional to a difference vector $\Delta\mathbf{R}(t) = \mathbf{R}_1(t) - \mathbf{R}_2(t)$, with $\mathbf{R}_1$ and $\mathbf{R}_2$ being vectors that connect the chain ends and the n^*th segment ($\mathbf{R}_1 + \mathbf{R}_2$ = end-to-end vector $\mathbf{R}$). Thus, a normalized relaxation function is given by an autocorrelation function of $\Delta\mathbf{R}$, $\Phi(t;n^*) = \langle\Delta\mathbf{R}(t)\cdot\Delta\mathbf{R}(0)\rangle/\langle\Delta R^2\rangle$. Representing Φ in terms of the local correlation function C (eq 1) and performing Fourier transformation of $-\partial\Phi/\partial t$, we obtain an expression for the dielectric loss ϵ'' in terms of the relaxation times τ_p and integrated eigenfunctions F_p for eigenmodes of C. The result is identical to eq 4, except that the dielectric intensity g_p for the pth eigenmode is given by[14,19]

$$g_p(n^*) = \Delta\epsilon[2F_p(n^*) - F_p(N)]^2 \quad \text{(for dipole-inverted chains)} \quad (6)$$

with $\Delta\epsilon$ being the total dielectric intensity. Equation 6 involves eq 5 for the regular type-A chains as a special case of $n^* = 0$ or N. ($F_p(0) = 0$; cf. eq 3.)

With linear least-squares fitting methods explained in our previous paper,[14] the ϵ'' data are decomposed into contributions from dielectric modes and $g_p(n^*)$ are evaluated. Then, applying eq 6 to the $g_p(n^*)$ data and considering symmetries of the eigenfunctions ($F_p(n) = F_p(N) - F_p(N-n)$ for p = odd and $F_p(n) = F_p(N-n)$ for p = even),[14] we obtain F_p as

$$F_p(N/2) - F_p(n^*) = \pm[g_p(n^*)/4\Delta\epsilon]^{1/2};\quad p = \text{odd} \quad (7a)$$

and

$$F_p(n^*) = \pm[g_p(n^*)/4\Delta\epsilon]^{1/2};\ p = \text{even} \quad (7b)$$

(When necessary, f_p are obtained as $(1/\sqrt{2})[\mathrm{d}F_p/\mathrm{d}(n^*/N)]$.) The sign in the right-hand sides of eq 7 is determined from a requirement of smooth and continuous n^* dependence of $F_p(n^*)$ for the series of dipole-inverted PI chains having narrowly spanned n^* values (cf. Table 1). Note that F_p's satisfy a relationship

$$\sum_{p=1}^{N} F_p(n)\,F_p(m) = n/N \text{ (for } n \le m) \text{ and } m/N \text{ (for } n > m) \quad (8)$$

that corresponds to an initial condition for the local correlation function,[14,19] $C(n,0;m) = \delta_{nm}$.

Table 1. Characteristics of PI and OB Samples

code	$10^{-3}M$	M_w/M_n	n^*/N^c	precursors molecular weights[d] $10^{-3}M_1{}^a$	$10^{-3}M_2{}^a$
Dipole-Inverted PI Chains[e]					
I-I 49-0[f]	48.8[a]	1.05	0	48.8	
I-I 50-6	55.4[a]	1.06	0.109	49.9	6.12
I-I 35-9	44.4[a]	1.05	0.213	35.0	9.48
I-I 35-14	47.6[a]	1.07	0.283	34.7	13.7
I-I 33-16	48.9[a]	1.07	0.325	32.6	15.7
I-I 28-18	47.4[a]	1.06	0.396	27.5	18.0
I-I 24-24[g]	47.7[a]	1.06	0.5	23.9	
Butadiene Oligomer					
OB-0.7	0.711[b]	1.08			

[a] Weight-average molecular weight. [b] Number-average molecular weight. [c] Reduced location of dipole-inversion point. [d] $M_w/M_n \le 1.08$ for all precursor PI's. [e] cis:trans:vinyl ≅ 75:20:5. [f] Without dipole inversion (inversion at the chain end). [g] With symmetrically inverted dipoles.

III. Experimental Section

III-1. Materials. Table 1 summarizes molecular characteristics of the dipole-inverted PI chains and a butadiene oligomer (OB-0.7) used in this study. The OB-0.7 sample was anionically synthesized with *tert*-butyllithium in benzene. The number-average molecular weight was determined from ^{1}H-NMR (by counting the proton numbers for the *tert*-butyl groups and butadiene monomer units in the sample), and the heterogeneity index M_w/M_n was determined from oligo-GPC.

The PI chains having inverted type-A dipoles were synthesized via a multistep coupling method and fully characterized in our previous study.[14] Details of the synthesis and characterization were described elsewhere.[14] The PI chains were composed of two PI blocks connected in a head-to-head fashion, and the dipole direction is the same in each block but inverted at the block junction. The sample code numbers for those PI chains indicate molecular weights of the two blocks in units of 1000. As seen in Table 1, the PI chains have nearly the same M (≅48K) but differently inverted dipoles that are specified by the reduced location of the inversion point, n^*/N.

III-2. Measurements. Homogeneous PI/OB-0.7 solutions with the PI concentration c_{PI} = 0.027, 0.045, 0.135, and 0.272 g cm^{-3} were prepared by first dissolving prescribed amounts of the PI and OB-0.7 samples in cyclohexane and then completely removing cyclohexane. (These c_{PI} values were calculated from a known weight fraction of PI under an assumption of no volume change on mixing.) Dielectric losses ϵ'' were measured for the PI/OB-0.7 solutions at temperatures (T) between −30 and +50 °C. (These T were well above T_g of the solutions.) The measurements were carried out with capacitance bridges (GR 1615A, General Radio; Precision LCR-meter 4284A, Hewlett-Packard) at angular frequencies ω (s^{-1}) ranging from 0.2K to 1.3M and ϵ'' were determined with accuracy better than 5%. The solvent, OB-0.7, had negligibly small ϵ'' at ω examined, and ϵ'' of the PI/OB-0.7 solutions were attributed to global motion of the PI chains.

The time−temperature superposition worked very well for the ϵ'' data at respective c_{PI}, and the data were reduced at a reference temperature T_r = 40 °C. In the T-range examined, the shift factor a_T exhibited rather small changes with T for all PI/OB-0.7 solutions: $-1 < \log a_T < 2.5$ for the largest change observed. Thus, all ϵ'' data at $T \neq T_r$ had sufficiently large overlapping with the data at T_r in the reduced frequency (ωa_T) scales. This large overlapping enabled us to construct the ϵ'' master curves with negligibly small uncertainties (<10% in the frequency scales shown later in Figure 4).

As seen from eq 6, dielectric intensities for the eigenmodes of the local correlation function are dependent on the location of the dipole-inversion point, and the slowest eigenmode (p = 1) does not necessarily have the maximum intensity. In particular, for the PI chain having symmetrically inverted dipoles (I-I 24-24 listed in Table 1), the dielectric intensities vanish for all odd modes and τ_1 cannot be evaluated from its ϵ'' data. For evaluation of τ_1 for the dipole-inverted PI chains, dielectric measurements were carried out for OB-0.7 solutions of monodisperse, *regular* PI chains (without dipole inversion) at concentrations c_{PI} = 0.027, 0.045, 0.135, and 0.272 g cm^{-3}. The molecular weights of those regular PI chains were chosen in a range (M = 35K−60K) that covered M's for the dipole-inverted PI chains. (One of the regular PI chains was the I-I 49-0 chain listed in Table 1.) The regular PI chains exhibited sharp ϵ'' peaks corresponding to the slowest eigenmodes, and τ_1 were evaluated as reciprocals of the peak frequencies. Those τ_1 data were interpolated and/or extrapolated to evaluate the τ_1 values for the dipole-inverted PI chains.

IV. Results

IV-1. Behavior of Regular PI Chains in OB-0.7. Figure 1 shows the dependence of τ_1 of regular PI chains in the OB-0.7 solutions at 40 °C on their molecular weights M_{PI} (large unfilled symbols). As explained earlier, the regular PI chains exhibited sharp ϵ'' peaks corresponding to the slowest eigenmode of the local correlation function, and their τ_1 were determined from the peak frequencies. Those τ_1 data were interpolated and/or extrapolated to evaluate τ_1 for the dipole-inverted PI chains (small filled symbols).

In the ranges of M_{PI} and c_{PI} examined in Figure 1, the M_{PI} dependence of τ_1 (large symbols) can be represented by a power-law relationship, $\tau_1 \propto M_{PI}^{\beta}$ (solid lines in the figure), with the exponent β = 1.65, 1.72, 2.18, and 3.5 for c_{PI} = 0.027, 0.045, 0.135, and 0.272 g cm^{-3}, respectively. Characteristic molecular weights for entanglement, M_c, are 33K and ≥67K for c_{PI} = 0.272 g cm^{-3} and $c_{PI} \leq$ 0.135 g cm^{-3}, respectively.[20] Thus, the PI chains examined are entangled at c_{PI} = 0.272 g cm^{-3} so that the well-known exponent, β = 3.5, is obtained. On the other hand, for $c_{PI} \leq$ 0.135 g cm^{-3}, the PI chains are in the nonentangled regime to exhibit much smaller β. In this regime β gradually decreases with decreasing c_{PI}, as found also for solutions in the usual solvents. In particular, the exponent for the dilute PI/OB-0.7 solutions (c_{PI} = 0.027 g cm^{-3}), β = 1.65, agrees well with the exponent found for dilute PI solutions in Isopar-G[11] (β = 1.69) and in heptane[13] (β = 1.63). This agreement suggests that the solubility for PI chains is nearly the same for OB-0.7 (the solvent used here), Isopar-G (used by Patel and Takahashi[11]), and heptane (used by Urakawa et al.[13]). These solvents are classified as moderately good (marginal) solvents for PI.

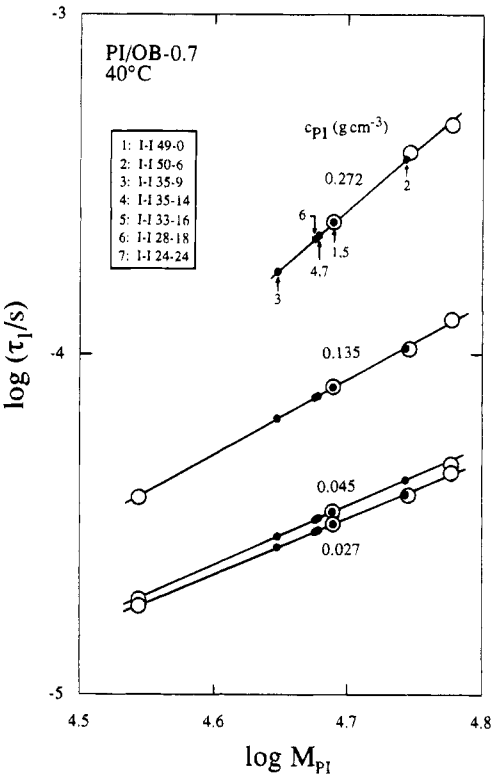

Figure 1. Molecular weight dependence of the longest relaxation time τ_1 at 40 °C for regular PI chains (without dipole inversion) in OB-0.7 (large symbols). The small symbols indicate τ_1 for the dipole-inverted PI chains evaluated from short interpolation/extrapolation of the τ_1 data for the regular PI chains.

We now focus our attention on the behavior of one particular PI chain examined in Figure 1, I-I 49-0 with M_{PI} = 48.8K (cf. Table 1). Figure 2 shows the c_{PI} dependence of the total dielectric intensity for the global relaxation, $\Delta\epsilon$, for I-I 49-0 in OB-0.7. We note that $\Delta\epsilon$ increases in proportion to c_{PI} for $c_{PI} \leq$ 0.045 g cm^{-3} and the c_{PI} dependence becomes slightly weaker for c_{PI} > 0.045 g cm^{-3}. Since $\Delta\epsilon$ is proportional to $c_{PI}\langle R^2\rangle/M_{PI}$, with $\langle R^2\rangle$ being the mean-square end-to-end distance,[7,12] this change in the c_{PI} dependence indicates that the excluded-volume interaction expands dilute PI chains in OB-0.7, as is the case also in Isopar-G[11] and heptane.[12]

A reduced intensity, $\Delta\epsilon^* = \Delta\epsilon/c_{PI}$, is proportional to $\langle R^2\rangle$. Thus, a ratio of $\Delta\epsilon^*$ at small c_{PI} to that in bulk state can be used as an expansion factor for $\langle R^2\rangle$ of dilute chains, $\alpha^2 = \langle R^2\rangle/\langle R_\theta^2\rangle$, with $\langle R_\theta^2\rangle$ being $\langle R^2\rangle$ in the unperturbed (bulk) state. In Figure 2, the α factor for

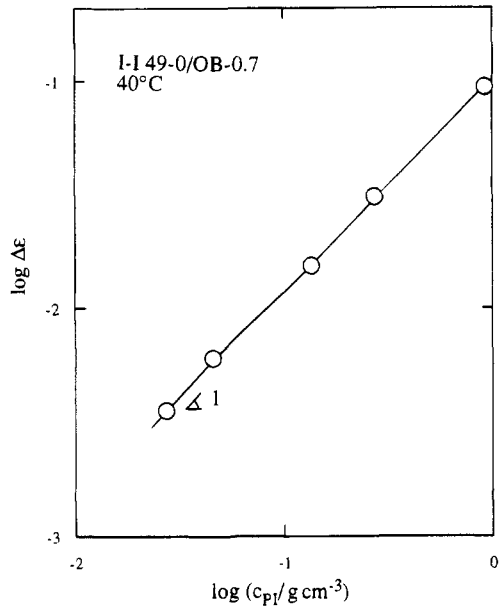

Figure 2. Concentration dependence of the dielectric intensity $\Delta\epsilon$ at 40 °C for the I-I 49-0 chain in OB-0.7. For comparison, $\Delta\epsilon$ is shown also for bulk I-I 49-0 (c_{PI} = 0.92 g cm^{-3}; bulk density).[14]

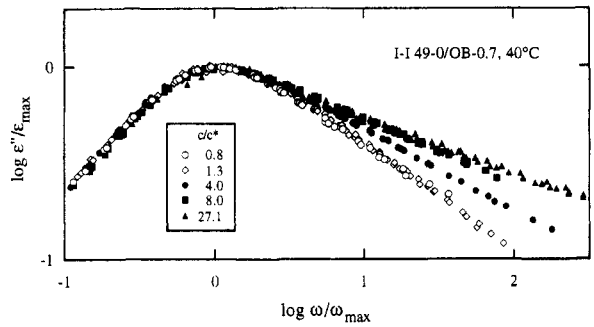

Figure 3. Comparison of the ϵ'' curves reduced at peaks for the I-I 49-0/OB-0.7 solutions with various PI concentrations as indicated.

the dilute I-I 49-0 chains (with c_{PI} = 0.027 g cm^{-3}) is evaluated to be 1.12. From this factor and the unperturbed radius of gyration for PI, $R_{g,\theta} = 0.335M_{PI}^{0.5}$ (Å),[22] we can evaluate R_g of I-I 49-0 in the dilute OB-0.7 solution, $R_g = \alpha R_{g,\theta} = 83$ Å, and further the overlapping threshold c^*,

$$c^* = [M_{PI}/N_A][4\pi R_g^3/3]^{-1} = 0.034 \text{ g cm}^{-3} \quad (N_A = \text{Avogadro's number}) \quad \text{for I-I 49-0/OB-0.7} \quad (9)$$

(In the above evaluation of R_g, we have neglected a small difference between expansion factors for $\langle R^2\rangle^{1/2}$ and R_g. This difference was found to be only 5% for PI chains in heptane[23] and is expected to be as small as 5% in OB-0.7 having nearly the same solubility for PI.)

Figure 3 shows changes of the ϵ'' curve for the I-I 49-0/OB-0.7 solution with c_{PI}. As done in previous studies,[13,13] comparison is made for the ϵ'' curves reduced at their peaks. The dielectric mode distribution is reflected in the shape (ω dependence) of those reduced ϵ'' curves. As seen in Figure 3, the distribution is rather sharp and hardly dependent on c_{PI} for $c_{PI} \leq 1.3c^*$, with c^* being the overlapping threshold (eq 9). With increasing c_{PI} up to $8c^*$, the distribution becomes broadened, and for $c_{PI} \geq 8c^*$ the broad distribution becomes independent of c_{PI}. These results are quite similar to those found for PI solutions in Isopar-G[11] and heptane.[13]

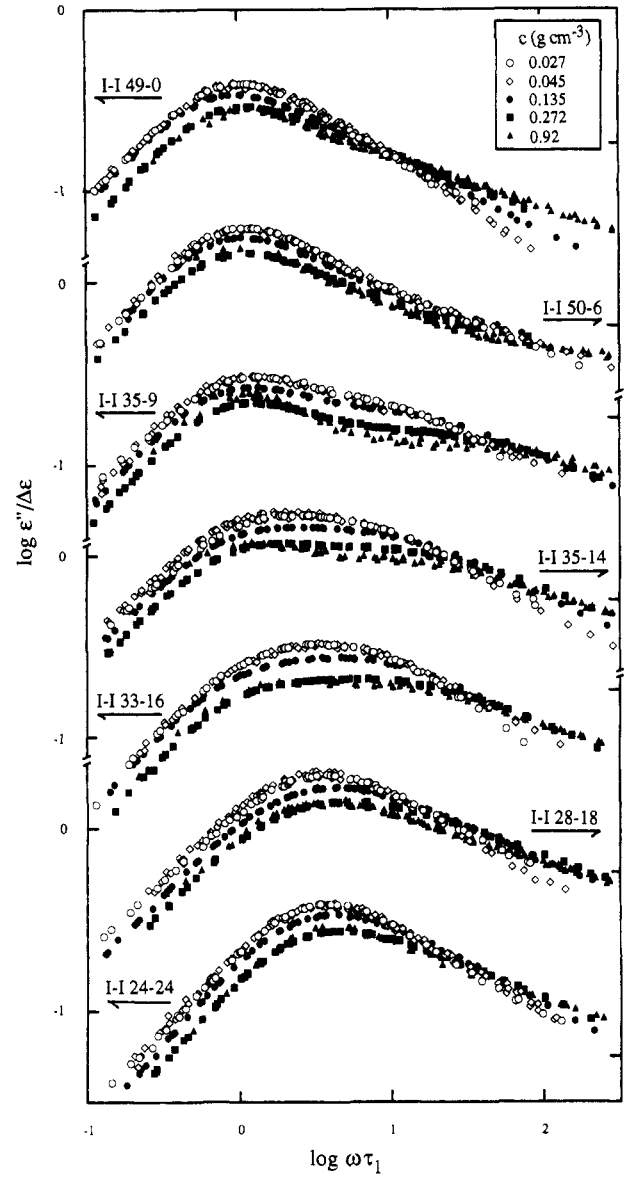

Figure 4. Dependence of normalized dielectric loss, $\epsilon''/\Delta\epsilon$, on reduced frequency, $\omega\tau_1$, for OB-0.7 solutions of the dipole-inverted PI chains with the concentrations as indicated.

As seen in Figures 1–3, the dielectric behavior of regular PI chains in OB-0.7 is essentially the same as the behavior in Isopar-G and heptane studied in previous papers.[11–13] Thus, the broadening of the dielectric mode distribution in these three solvents should have a common origin, that is discussed in later sections in relation to the behavior of dipole-inverted PI chains in OB-0.7.

IV-2. ϵ'' Curves for Dipole-Inverted PI Chains in OB-0.7. Figure 4 shows ϵ'' curves at 40 °C for the OB-0.7 solutions of the dipole-inverted PI chains (Table 1). Differing from Figure 3, Figure 4 shows normalized dielectric loss, $\epsilon''/\Delta\epsilon$, plotted against reduced frequencies $\omega\tau_1$. At respective c_{PI}, good agreement of the $\Delta\epsilon$ values was found for the dipole-inverted PI chains including I-I 49-0 (cf. Figure 2). τ_1 for the dipole-inverted chains were evaluated in Figure 1 (small symbols). Those τ_1 values, obtained after short interpolation/extrapolation, contain negligibly small uncertainties.

The seven dipole-inverted PI chains have almost identical M_{PI} (≅48K; cf. Table 1) and thus almost identical c^*. Therefore, in the reduced frequency scale shown in Figure 4, we can consider the global motion

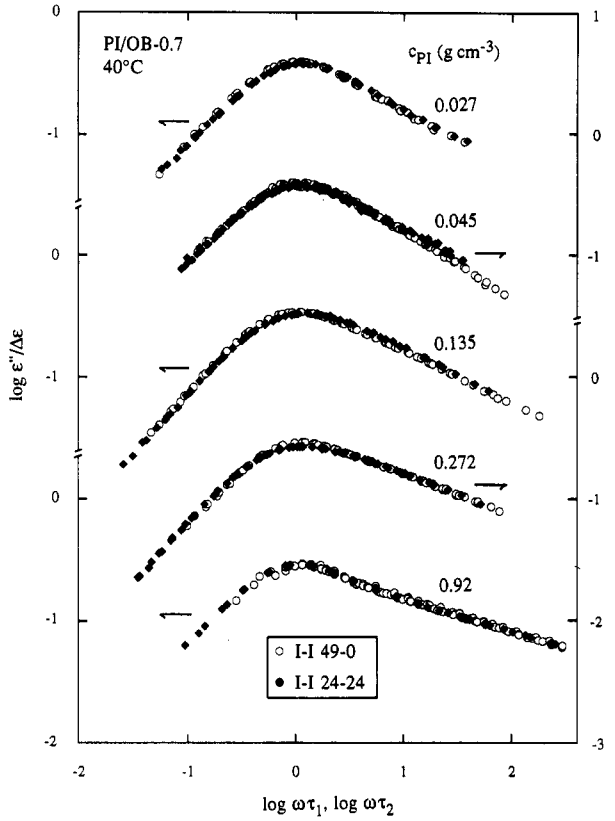

Figure 5. Comparison of the $\epsilon''/\Delta\epsilon$ curves for I-I 49-0 (without dipole inversion) and 24-24 (with symmetrical inversion) in OB-0.7 solutions. The $\epsilon''/\Delta\epsilon$ data are plotted against $\omega\tau_1$ (for I-I 49-0) and $\omega\tau_2$ (for I-I 24-24).

and the time evolution of the local correlation function (eq 1) to be exactly the same for those PI chains. Nevertheless, at respective c_{PI}, the PI chains exhibit significantly different dielectric relaxation behavior: As seen in Figure 4, the ϵ'' curves are first broadened and then become narrow again as the dipole-inversion point shifts from the chain end to the chain center. These changes correspond to the n^* dependence of the dielectric intensities g_p for the eigenmodes (eq 6). In particular, the I-I 24-24 ($n^*/N = 1/2$) and I-I 49-0 ($n^*/N = 0$) chains exhibit almost indistinguishable shapes of the ϵ'' curves, as demonstrated in Figure 5 where $\epsilon''/\Delta\epsilon$ is plotted against $\omega\tau_2$ (for I-I 24-24) and/or $\omega\tau_1$ (for I-I 49-0). (Here, τ_2 is the relaxation time for the second eigenmode shown later in Figure 7: τ_2 were evaluated from ϵ'' peak frequencies for I-I 24-24).

More importantly, we also note in Figure 4 for each dipole-inverted chain that the dielectric mode distribution is broadened with increasing c_{PI}. Close inspection reveals that the broadening corresponds to a decrease in the $\epsilon''/\Delta\epsilon$ peak height with c_{PI} and an increase in the magnitude of $\epsilon''/\Delta\epsilon$ at high ω. As discussed later, this broadening is further related to changes in F_p with c_{PI}.

In Figure 6, the $\epsilon''/\Delta\epsilon$ curves of the dipole-inverted PI chains in the dilute OB-0.7 solutions (c_{PI} = 0.027 g cm^{-3}) are compared with predictions of the free-draining Rouse (dashed curves), nondraining Zimm (dash-dot curves), and nondraining Tschoegl (solid curves) models.[24-26] The excluded-volume (EV) interaction, not considered in the Rouse and Zimm models, is incorporated in the Tschoegl model through a scheme of uniform chain expansion, and the EV parameter of this model used in Figure 6 is ϵ = 0.2.[27] These models predict the same sinusoidal eigenfunctions (within the approximations involved in respective models)[24]

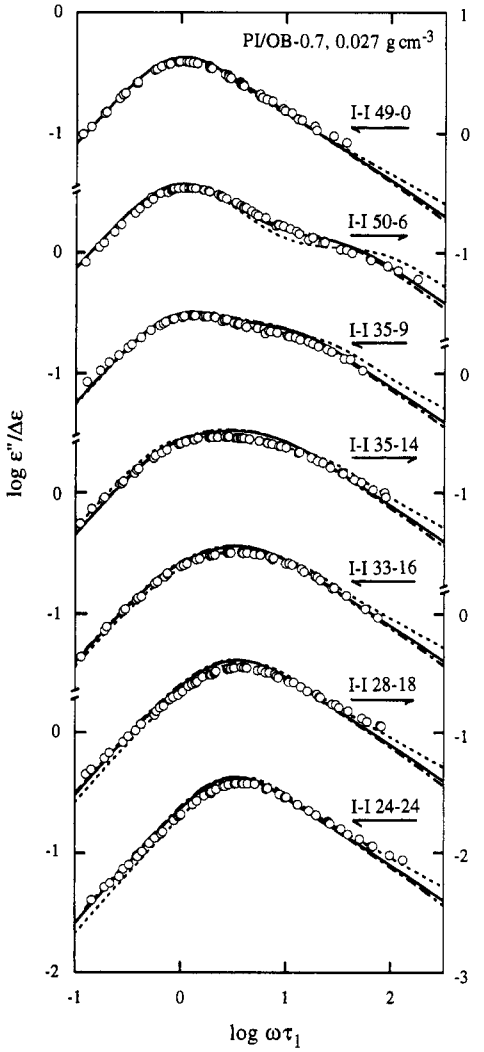

Figure 6. Comparison of the $\epsilon''/\Delta\epsilon$ curves (symbols) for the dilute dipole-inverted PI chains in OB-0.7 (c_{PI} = 0.027 g cm^{-3}) with the prediction of the Rouse (dashed curves), Zimm (dash-dot curves), and Tschoegl (ϵ = 0.2; solid curves) models.

$$F_p^\circ(n) = \frac{\sqrt{2}}{p\pi}\left[1 - \cos\frac{p\pi n}{N}\right], \quad f_p^\circ(n) = \sin\frac{p\pi n}{N} \quad (10)$$

Thus, the dielectric intensities for the eigenmodes are the same for the three models (cf. eq 6). However, a span of the relaxation times τ_p is different: In a continuous limit, the τ_p span is[24-26]

$$\text{Rouse:} \quad \tau_p/\tau_1 = p^{-2} = 1/4\ (p = 2),\ 1/9\ (p = 3),\ \ldots \quad (11)$$

$$\text{Zimm:} \quad \tau_p/\tau_1 = 1/3.17\ (p = 2),\ 1/5.99\ (p = 3),\ \ldots,\ 0.819p^{-1.5}\ (\text{for } p \gg 1) \quad (12)$$

$$\text{Tschoegl } (\epsilon = 0.2): \quad \tau_p/\tau_1 = 1/3.31\ (p = 2),\ 1/6.48\ (p = 3),\ \ldots,\ 0.853p^{-1.6}\ (\text{for } p \gg 1) \quad (13)$$

These differences lead to the differences seen for the dashed, dash-dot, and solid curves in Figure 6.

As seen in Figure 6, *at low* ω the three models predict almost identical shapes for the ϵ'' curve of the I-I 49-0 chain (without dipole inversion) because the predicted curves are in any way dominated by the slowest eigenmode. Thus, it is difficult to distinguish those models from the shape of the ϵ'' curve for this chain (as were the cases also for regular PI chains examined in previous studies[11,13]). However, differences between the

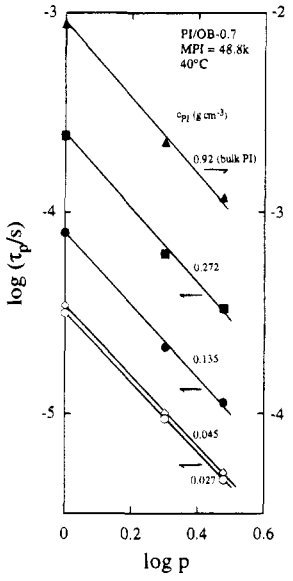

Figure 7. Dependence of the relaxation times τ_p for eigenmodes of I-I 49-0 at 40 °C on the mode index p. The I-I 49-0 concentration is varied from 0.027 to 0.92 g cm^{-3}.

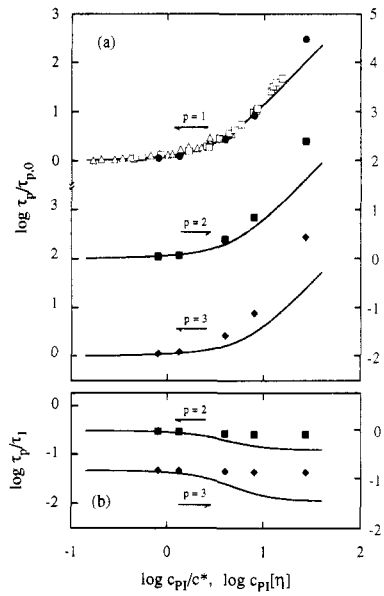

Figure 8. Concentration dependence of (a) $\tau_p/\tau_{p,0}$ ratios and (b) τ_p/τ_1 ratios at 40 °C for the I-I 49-0 chain in OB-0.7 (filled symbols). The unfilled triangles and squares indicate the $\tau_1/\tau_{1,0}$ ratios obtained by Patel and Takahashi[11] (for PI/Isopar-G solutions with M_{PI} = 31K−1.3M and $c_{PI} \leq 8\%$) and by Urakawa et al.[13] (for PI/heptane solutions with M_{PI} = 140K and 747K and $c_{PI} \leq 0.178$ g cm^{-3}), respectively. The solid curves indicate the prediction of the Muthukumar theory[18] with the parameters evaluated by Urakawa et al.[13]

models become prominent for the dipole-inverted chains, and the data are close to the predictions of the Zimm and Tschoegl models, with a small preference for the latter (cf. ϵ'' curves for I-I 50-6). This result indicates the well-known importance of the hydrodynamic and excluded-volume interactions for dynamics of dilute chains.

IV-3. Dependence of Relaxation Times τ_p on p and c_{PI}. From the ϵ'' data for the I-I 49-0 and I-I 24-24 solutions, the relaxation times τ_p were evaluated for the lowest three eigenmodes of the local correlation function. As seen from eq 6, all even eigenmodes dielectrically vanish for the I-I 49-0 chain ($n^* = 0$), while all odd eigenmodes vanish for the I-I 24-24 chain ($n^* = N/2$). Thus, sharp ϵ'' peaks observed for the I-I 49-0 and I-I 24-24 chains (cf. Figures 4 and 5) correspond to the first and second eigenmodes, respectively, and τ_1 and τ_2 for the respective chains were evaluated from their peak frequencies. τ_2 for I-I 49-0 was obtained after a minor correction for the small M_{PI} difference between I-I 49-0 and I-I 24-24 (M_{PI} = 48.8K and 47.7K). τ_3 was evaluated from the ϵ'' data for I-I 49-0 with a previously reported linear least-squares fitting method.[14]

Figure 7 shows dependence of the relaxation times τ_p for the I-I 49-0 chain at respective c_{PI} on the eigenmode index p (=1−3). The p dependence becomes a little stronger with increasing c_{PI}. If we *approximate* this dependence (for $p \leq 3$) with a power-law relationship, $\tau_p \propto p^{-\gamma}$ (solid lines in the figure), the exponent γ is evaluated to be 1.75, 1.77, 1.82, 1.87, and 1.92 for c_{PI} (g cm^{-3}) = 0.027, 0.045, 0.135, 0.272, and 0.92 (bulk state). In the dilute solution (c_{PI} = 0.027 g cm^{-3}) the p dependence of τ_p is reasonably described by the Tschoegl model (ϵ = 0.2; eq 13), and in the concentrated solutions the dependence approaches the prediction of the Rouse and reptation models[25] ($\tau_p \propto p^{-2}$). In particular, the observed τ_2/τ_1 ratio (=1/3.9) for c_{PI} = 0.272 and 0.92 g cm^{-3} is very close to the model prediction, $\tau_2/\tau_1 = 1/4$.

We now focus our attention on the c_{PI} dependence of τ_p. Patel and Takahashi[11] and Urakawa et al.[13] found a universal relationship between $\tau_1/\tau_{1,0}$ and $c_{PI}[\eta]$ for semidilute solutions of regular PI chains in Isopar-G and heptane, with $\tau_{1,0}$ and $[\eta]$ being τ_1 at infinite dilution and the intrinsic viscosity, respectively. The product, $c_{PI}[\eta]$, is a measure for the chain overlapping, and the universal relationship suggests that the degree of chain overlapping determines the magnitude of retardation of the PI relaxation with increasing c_{PI}. The degree of chain overlapping is also represented by a c_{PI}/c^* ratio, with the overlapping threshold $c^* = [M_{PI}/N_A][4\pi R_g^3/3]^{-1}$ being evaluated in eq 9 for the I-I 49-0 chain in OB-0.7. Thus, we evaluated $\tau_{p,0}$ (p = 1−3) by extrapolating the τ_p data for I-I 49-0 (Figure 7) to c_{PI} = 0 and examined the dependence of $\tau_p/\tau_{p,0}$ on c_{PI}/c^*. The results are shown in part a of Figure 8 (filled symbols). Unfilled symbols indicate the dependence of $\tau_1/\tau_{1,0}$ on $c_{PI}[\eta]$ found in previous studies,[11,13] and the solid curves, prediction of the Muthukumar theory[18] discussed in a later section.

As seen in Figure 8a, the $\tau_1/\tau_{1,0}$ ratio increases monotonically with c_{PI}/c^* for I-I 49-0 in OB-0.7. This c_{PI}/c^* dependence agrees well with the $c_{PI}[\eta]$ dependence of $\tau_1/\tau_{1,0}$ for PI chains in Isopar-G[11] (unfilled triangles) and heptane[13] (unfilled squares), again indicating that the relaxation behavior of PI chains is the same in these solvents (within small differences between $[\eta]$ and $1/c^*$). More importantly, Figure 8a indicates that $\tau_2/\tau_{2,0}$ and $\tau_3/\tau_{3,0}$ ratios also increase with c_{PI}/c^* and closely follow the change in $\tau_1/\tau_{1,0}$. This behavior is most clearly seen in part b of Figure 8, where the c_{PI}/c^* dependence is examined for τ_2/τ_1 and τ_3/τ_1 ratios (relaxation time span). These ratios exhibit only a weak c_{PI}/c^* dependence, meaning that the c_{PI} dependence is nearly the same for τ_1, τ_2, and τ_3. (This result corresponds to the very gradual increase of the exponent γ seen in Figure 7.)

IV-4. Changes of Eigenfunctions with c_{PI}. Fitting the ϵ'' data for the dipole-inverted PI chains (Figure 4) with low-ω forms of eq 4,

$$\epsilon''(\omega;n^*) = g_1(n^*)\, D_1(\omega) + g_2(n^*)\, D_2(\omega) + G_3(n^*)\, \omega \qquad (14)$$

and

$$\epsilon''(\omega;n^*) = g_1(n^*)\,D_1(\omega) + g_2(n^*)\,D_2(\omega) + g_3(n^*)\,D_3(\omega) + G_4(n^*)\,\omega \quad (15)$$

we can decompose the data into contributions of eigenmodes and evaluate the dielectric intensities, $g_1 - g_3$, for the lowest three eigenmodes. Here, $D_p(\omega) = \omega\tau_p/(1 + \omega^2\tau_p^2)$ is the single relaxation function for the pth eigenmode, and $G_q(n^*)$ ($q = 3, 4$) is the low-ω asymptote of the contribution $\epsilon_{(\geq q)}''$ from all kth eigenmodes with $k \geq q$,

$$\epsilon_{(\geq q)}'' = \sum_{k \geq q} g_k(n^*)\,D_k(\omega) \quad (16)$$

The $\tau_1 - \tau_3$ values specifying the location of $D_1(\omega) - D_3(\omega)$ have been determined for I-I 49-0 (Figure 7), and those values for the other dipole-inverted chains were obtained after a minor correction for small M_{PI} differences (by use of the data in Figure 1). Thus, for those PI chains, eqs 14 and 15 are linear with respect to the unknown quantities, $g_1 - g_3$ (and G_3 and G_4), so that these quantities can be determined, with the highest accuracy attainable, from standard, linear least-squares fits of the ϵ'' data at low ω with eqs 14 and 15. Details of fitting procedures were described previously.[14]

As an example, Figure 9 shows results of the fit with eq 15 for the PI/OB-0.7 solutions of $c_{PI} = 0.027$ g/cm^{-3}. A similar quality of fit was obtained also for the solutions of other c_{PI}. In Figure 9 the unfilled symbols indicate the ϵ'' data, and the thin dash-dot, dashed, and solid curves indicate the contributions from the lowest three eigenmodes, g_1D_1, g_2D_2, and g_3D_3, respectively. The filled symbols indicate the higher mode contribution, $\epsilon_{(\geq 4)}''$ (eq 16). The prerequisite of the fit, $\epsilon_{(\geq 4)}'' \propto \omega$ (eq 15), is well satisfied at low ω ($<10/\tau_1$), and the mode decomposition is well achieved. A similar quality of fit was obtained also for eq 14, and the g_1 and g_2 values obtained from the fit with eq 14 were very close to those with eq 15.

From the $g_1 - g_3$ values thus obtained, we evaluated the integrated eigenfunctions, $F_1 - F_3$ (eq 7). Figure 10 examines dependence of these F_p on the reduced segment location, n/N, at concentrations $c_{PI}/c^* = 0.8$, 4.0, and 8.0 ($c_{PI} = 0.027$, 0.135, and 0.272 g cm^{-3}). F_p for $c_{PI}/c^* = 1.3$ and 27.1 (not shown here for simplicity of the figure) were close to those for $c_{PI}/c^* = 0.8$ and 8.0, respectively. Most of the models so far proposed, e.g., Rouse, Zimm, Tschoegl, and reptation models, have sinusoidal F_p° (eq 10). For convenience of comparing the experimental F_p and model F_p°, Figure 10 shows $\Delta F_p(n) = F_p(n) - F_p(N/2)$ ($p = 1-3$), not $F_p(n)$ themselves. The thin, solid curves indicate $\Delta F_p^\circ(n)$ for the models,

$$\Delta F_p^\circ(n) = \frac{\sqrt{2}}{p\pi}\left[\cos\frac{p\pi}{2} - \cos\frac{p\pi n}{N}\right] \quad (17)$$

F_p and F_p° (and thus ΔF_p and ΔF_p° too) are normalized according to eq 8. Thus, in Figure 10 we can compare both n dependence and absolute magnitudes for F_p and F_p°.

As seen in Figure 10, the experimental $\Delta F_p(n)$ for dilute PI chains ($c_{PI}/c^* = 0.8$) are nearly sinusoidal with respect to n/N and reasonably close to the model $\Delta F_p^\circ(n)$, in particular for $p = 1$. However, with increasing c_{PI}/c^*, $\Delta F_p(n)$ deviate from $\Delta F_p^\circ(n)$ and their nonsinusoidal n dependence becomes more prominent. As shown later in Figure 12, these changes of F_p correspond to changes in the dielectric intensities for the eigenmodes of the local correlation function.

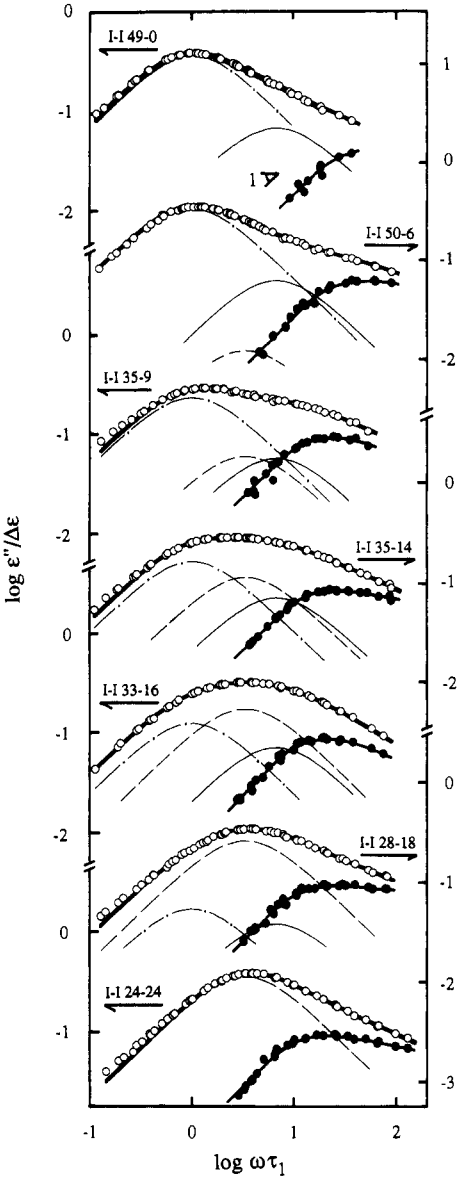

Figure 9. Results of the mode decomposition of the ϵ'' data (unfilled symbols) by fit with eq 15 for the dipole-inverted PI chains in OB-0.7 ($c_{PI} = 0.027$ g cm^{-3}). The thin dash-dot, dashed, and solid curves indicate the contributions from the first to third eigenmodes, $g_pD_p(\omega)$ with $p = 1-3$. The higher mode contribution, $\epsilon_{(\geq 4)}''$ (eq 16), is indicated with the filled symbols. The thick solid curves indicate the recalculated $\epsilon'' = g_1D_1 + g_2D_2 + g_3D_3 + \bar{\epsilon}_{(\geq 4)}''$, with $\bar{\epsilon}_{(\geq 4)}''$ being evaluated for the solid curves that smoothly connect the filled symbols.

To quantify the changes of F_p seen in Figure 10, we expanded F_p with respect to F_p° as

$$F_p(n) = \sum_i a_{pi}F_i^\circ(n) \quad (18)$$

and evaluated the expansion coefficients a_{pi} from Fourier analysis for the F_p data. Figure 11 shows the c_{PI} dependence of the coefficients. F_1 and F_2 gradually vary with n/N (Figure 10), and their coefficients, a_{1i} (top panel) and a_{2i} (middle panel), were accurately evaluated. On the other hand, F_3 rather rapidly varies with n/N (in particular at $n/N \cong 0$ and 1) so that the limited number of data points unavoidably introduced some uncertainty in the evaluated coefficients a_{3i} (bottom panel). However, those coefficients are still useful for quantifying the changes of F_3 with c_{PI}.

As seen in Figure 11, the diagonal coefficients for F_1 and F_2, a_{11} and a_{22}, respectively, monotonically increase

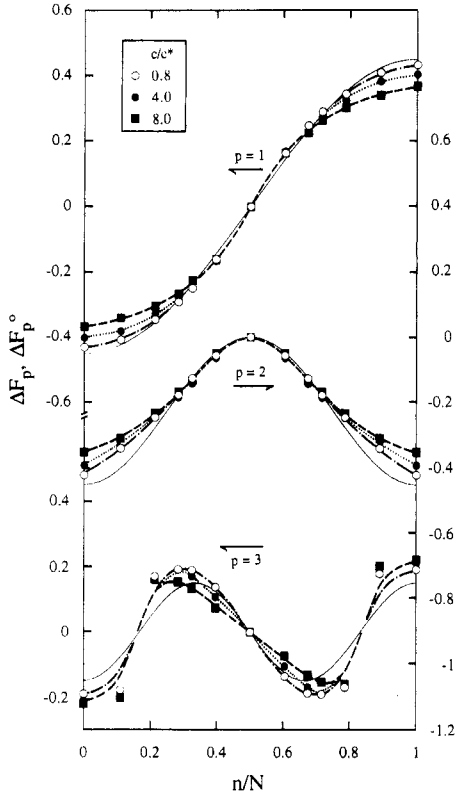

Figure 10. Plots of $\Delta F_p(n) = F_p(n) - F_p(N/2)$ $(p = 1-3)$ against n/N for the PI chains in OB-0.7 (symbols). The thin, solid curves indicate $\Delta F_p^\circ(n) = [\sqrt{2}/p\pi][\cos(p\pi/2) - \cos(p\pi n/N)]$ predicted from the Zimm, Rouse, Tschoegl, and reptation models. Note that ΔF_p and ΔF_p° are normalized according to eq 8.

and appear to approach unity with decreasing c_{PI}, while a_{33} for F_3 appears to approach unity after exhibiting a maximum. We also note that all off-diagonal coefficients, a_{pi} with $i \neq p$, approach zero with decreasing c_{PI}. A quantity, $Q_p = 1 - a_{pp}/[\sum_i a_{pi}^2]^{1/2}$, can be used as a measure for the difference between the observed F_p and sinusoidal F_p°, and those changes of a_{pi} quantitatively indicate that $Q_p \to 0$; i.e., the nonsinusoidal n dependence of F_p becomes less prominent with decreasing c_{PI}.

V. Discussion

V-1. Eigenmodes in Dilute Solutions. The PI chains in the dilute OB-0.7 solutions ($c_{PI} = 0.027$ g cm^{-3}) are subjected to both hydrodynamic (HD) and excluded-volume (EV) interaction (cf. Figure 2). Consequently, their dielectric behavior (Figures 1, 6, and 7) is better described by the Tschoegl model considering these interactions than by the Zimm model without the EV interaction: Although the shape of the ϵ'' curves is almost equally well described by the two models (Figure 6), the Zimm model fails to explain the observed M_{PI} and p dependence of the relaxation times at $c_{PI} = 0.027$ g cm^{-3}, $\tau_1 \propto M_{PI}^{1.65}$, $\tau_2/\tau_1 = 1/3.34$, and $\tau_3/\tau_1 = 1/6.75$ (Figures 1 and 7).[28]

Nevertheless, we note a small but nonnegligible disagreement between the data and the Tschoegl model: As can be seen in Figures 10 and 11, the experimental eigenfunctions F_p are nearly but not perfectly sinusoidal even at $c_{PI} = 0.027$ g cm^{-3} $(=0.8c^*)$ while the model has sinusoidal F_p° (eq 10).[24] This small disagreement might be related to a limitation of the uniform chain expansion scheme involved in the model and also to some small c_{PI} dependence of F_p that might

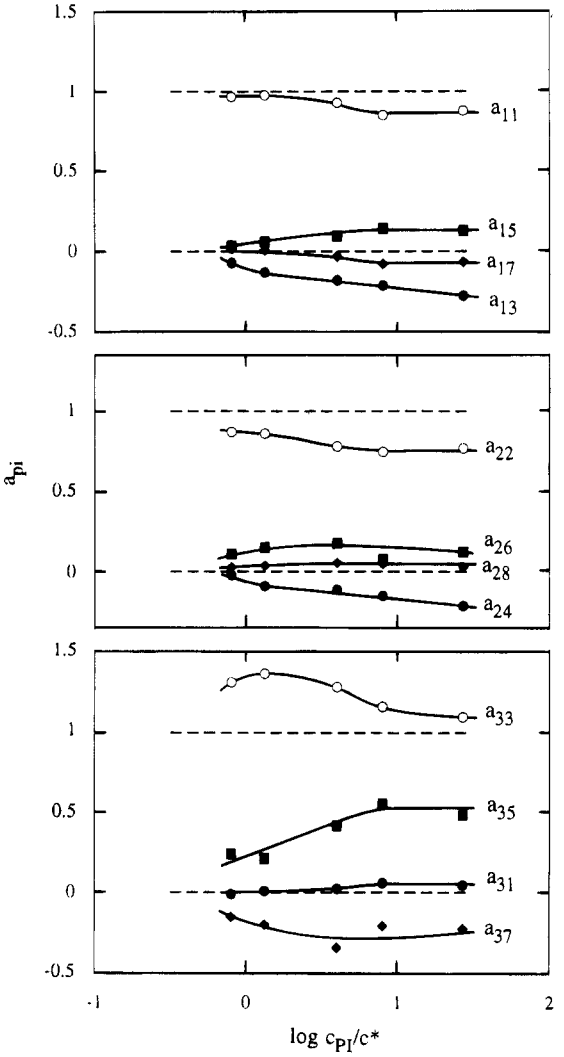

Figure 11. Concentration dependence of the Fourier expansion coefficients a_{pi} defined by eq 18 for the dipole-inverted PI chains in OB-0.7. The unfilled circles indicate the diagonal coefficients, a_{pp} $(p = 1-3)$, and the filled symbols denote the off-diagonal coefficients, a_{pi} with $p \neq i$.

survive at c_{PI} as small as $0.8c^*$. Further studies are desired for that disagreement. Concerning this problem, it would be interesting to examine the dielectric behavior of dipole-inverted chains in Θ solvents and test whether F_p are sinusoidal at c_{PI} as small as $0.8c^*$.

V-2. Changes of Dielectric Mode Distribution with c_{PI}. Figure 10 has demonstrated that the eigenfunctions F_p change their n dependence with increasing c_{PI}. These changes led to changes in the dielectric intensities for the eigenmodes. As an example, Figure 12 shows c_{PI} dependence of reduced intensities $g_1(0)/\Delta\epsilon$ and $g_3(0)/\Delta\epsilon$ (cf. eq 6) for the first and third eigenmodes of the I-I 49-0 chain. ($g_2(0) = 0$ for this chain.) The intensity $g_p(0)/\Delta\epsilon$ represents the fraction of orientational correlation memory that decays through the pth eigenmode. Two dashed lines indicate $g_p(0)/\Delta\epsilon$ $(=8/p^2\pi^2)$ for the Zimm, Rouse, Tschoegl, and reptation models (having the same F_p° given by eq 10).

As seen in Figure 12, $g_1(0)/\Delta\epsilon$ decreases significantly, while $g_3(0)/\Delta\epsilon$ increases a little with increasing c_{PI}. In particular, the decrease of $g_1(0)/\Delta\epsilon$ well corresponds to the decrease of the $\epsilon''/\Delta\epsilon$ peak height seen for I-I 49-0 (Figure 4). Thus, changes in F_p with c_{PI} (Figure 10) inducing the changes of $g_p(n^*)/\Delta\epsilon$ largely contribute to the broadening of the dielectric mode distribution. On

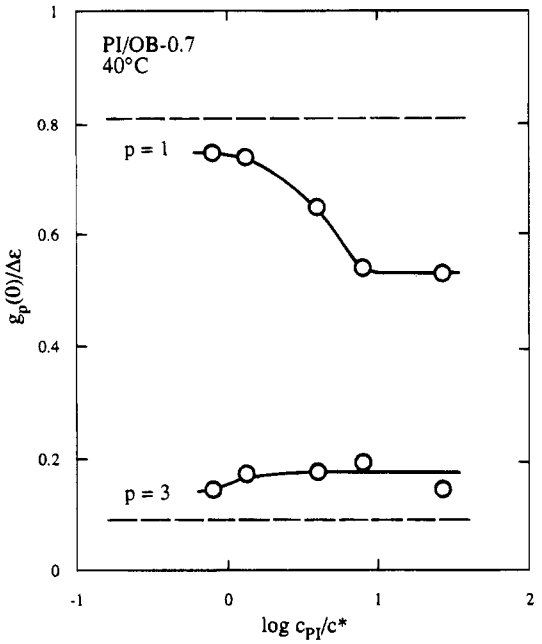

Figure 12. Concentration dependence of the reduced dielectric intensities for the first and third eigenmodes of the I-I 49-0 chain in OB-0.7. The dashed line indicate the intensities predicted from the Zimm, Rouse, Tschoegl, and reptation models.

the other hand, comparison of Figures 8b and 10 indicates that the changes in the relaxation time span (τ_p/τ_1) with c_{PI} are much less significant as compared to the changes in F_p. From this experimental fact, we can conclude that the broadening of the dielectric mode distribution for the regular and dipole-inverted chains (Figures 3 and 4) is essentially due to changes in F_p (Figure 10), not due to the small changes in the τ_p span (Figure 8b), at least at low ω where the lowest three eigenmodes dominate the dielectric relaxation.

Concerning the above conclusion, we note for concentrated PI solutions that the p dependence of τ_p (Figure 7) is very close to that for the Rouse and/or reptation models, but the observed ϵ'' curves are broader than the prediction (Figures 3 and 4). This disagreement for the observed and predicted shape of ϵ'' curves is due to the differences between the experimental F_p and model $F_p°$, again indicating that the broadened dielectric mode distribution is attributed to changes in F_p with c_{PI}.

Here, comments should be made for previous discussions for the concentration dependence of τ_1. Patel and Takahashi[11] compared their τ_1 data for PI/Isopar-G solutions with the Muthukumar theory[18] and reported a fair agreement, while Urakawa et al.[13] made a similar comparison for PI/heptane solutions and concluded that τ_1 of those solutions conforms well to the theory. The Muthukumar theory considers changes of the hydrodynamic and excluded-volume interactions with concentration, c. The predicted c dependence of τ_p is written as[18]

$$\tau_p/\tau_{p,0} = 1 + cAp^{-\kappa} - 2^{1/2}[cAp^{-\kappa}]^{3/2} + 2[cAp^{-\kappa}]^2 + ... \quad (19)$$

where A and κ are constants dependent on the strength of the excluded-volume interaction. (The Muthukumar–Freed theory[17] is involved in the Muthukumar theory[18] as a low-c asymptote.) As seen from eq 19, the Muthukumar theory predicts the *increase* of the relaxation time span (decrease of τ_p/τ_1 ratios) with increasing

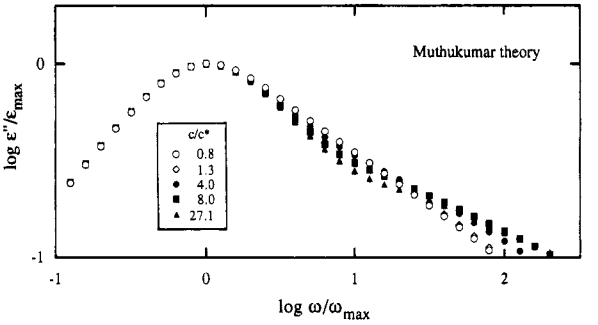

Figure 13. ϵ'' curves predicted from the Muthukumar theory[18] for the I-I 49-0 chain with concentrations as indicated. As done in Figure 3, the curves are reduced at their peaks. A small molecular weight distribution of the I-I 49-0 chain was neglected in the calculation.

c. Urakawa et al.[13] evaluated the Muthukumar parameters for their PI/heptane solutions as $A = 0.29[\eta]$ and $\kappa = 0.634$. The $\tau_p/\tau_{p,0}$ and τ_p/τ_1 ratios calculated from the Muthukumar theory with these parameters are indicated with the solid curves in parts a and b of Figure 8. As seen in Figure 8a, the theory reasonably describes the τ_1 data for PI/OB-0.7 solutions (filled circles) at $c_{PI} \leq 8c^*$. (Here, we have again neglected small differences between $[\eta]$ and c^*.) However, τ_2 and τ_3 increase with c_{PI} more rapidly than the prediction.

As explained earlier, the dipole-inverted PI chains are entangled at $c_{PI} \geq 8c^*$ (=0.272 g cm^{-3}) so that the rapid increase of $\tau_1 - \tau_3$ at $c_{PI} \geq 8c^*$ (Figure 8a) should be partly due to the entanglement effect. In addition, the segmental friction ζ should increase with c_{PI} to partly contribute the rapid increase of $\tau_1 - \tau_3$ at large c_{PI}. The Muthukumar theory does not consider the entanglement effect and the increase of ζ. Thus, for meaningful examination of the theory, the comparison with the data should be made in the nonentangled regime ($c_{PI} < 8c^*$) for the τ_p/τ_1 ratios that are not affected by the increase of ζ. As seen in Figure 8b, the Muthukumar theory predicts significant decreases of these ratios with increasing $c > c^*$, while the observed ratios are quite insensitive to c: For example, at $c_{PI} = 4c^*$, the model predicts $\tau_2/\tau_1 = 1/5.15$ and $\tau_3/\tau_1 = 1/12.67$, while the data are $\tau_2/\tau_1 = 1/3.72$ and $\tau_3/\tau_1 = 1/7.0$. From this fact, we can conclude that the theory does not describe the c dependence of the relaxation time span at $c > c^*$ where the broadening of the ϵ'' curves takes place.

In relation to this conclusion, Figure 13 shows the ϵ'' curves predicted from the Muthukumar theory for the I-I 49-0 chain at various c_{PI} as indicated. As done in Figure 3, the curves are reduced at their peaks. Within the approximation used in refs 17 and 18, the Muthukumar theory leads to sinusoidal $F_p°$ (eq 10) that give $g_p(0) = 8\Delta\epsilon/p^2\pi^2$ (p = odd) for the I-I 49-0 chain (cf. eq 6). The curves shown in Figure 13 were calculated from these g_p values together with the τ_p span specified by eq 19. As seen there, the theory predicts that the ϵ'' curve becomes sharper around its peak and broader at high-ω tail with increasing c. However, the data (Figure 3) do not exhibit such changes in both nonentangled ($c_{PI} < 8c^*$) and entangled ($c_{PI} \geq 8c^*$) states. This result again indicates that the changes of the eigenfunctions (and of $g_p/\Delta\epsilon$) are essential for the observed broadening of the ϵ'' curves.

The results seen in Figures 8 and 13 indicate the necessity of reexamining the recent conclusion of Adachi et al.[16] They studied dielectric behavior of a type-A chain, poly(ϵ-caprolactone) (PCL), in a marginal solvent (benzene) and concluded that the Muthukumar theory

is valid for describing the shape of ϵ'' curves up to c as large as $3c^*$ *if molecular weight distribution (MWD) of the chain is taken into account.* However, the behavior of PCL is quite similar to that of PI,[16] and for PI the theory does not describe the τ_p span at $c > c^*$ where the dielectric mode distribution is broadened (cf. Figure 8b). This fact strongly suggests that the agreement of the observed and calculated shape claimed by Adachi et al.[16] merely reflects the width of the *assumed* MWD but does not mean the validity of the theory.

V-3. Changes of Viscoelastic and OFB Mode Distribution with *c*. It is very interesting and important to compare the c dependence of the dielectric quantities with that of viscoelastic quantities[29,30] and oscillatory flow birefringence[31-33] (OFB). Extensive studies in the dilute to semidilute regime have suggested that the viscoelastic/OFB relaxation time $\tau_{p,\mathrm{OFB}}$ increases with c more rapidly for the slowest mode ($p = 1$) than for higher order modes ($p > 1$)[29-33] and that the corresponding increase in the $\tau_{p,\mathrm{OFB}}$ span causes the well-known Zimm-to-Rouse-like change of the viscoelastic mode distribution.[29,30] The dielectric $\tau_{p,\epsilon}$ span becomes *a little* wider with increasing c (from Tschoegl-like span to Rouse/reptation-like span; cf. Figures 7 and 8b). In this sense, the dielectric data are similar to the viscoelastic/OFB data. However, the $\tau_{p,\mathrm{OFB}}$ span has not been quantitatively evaluated even for the lowest few modes, and at this moment we cannot quantitatively compare the $\tau_{p,\mathrm{OFB}}$ span with the $\tau_{p,\epsilon}$ span ($p = 1-3$) determined in this study.

The c dependence of the *longest* viscoelastic/OFB relaxation time, $\tau_{1,\mathrm{OFB}}$, is described by the Muthukumar theory up to $c \cong 5c^*$ (or more; cf. Figure 5 of ref 33), as is the case also for the *longest* dielectric relaxation time, $\tau_{1,\epsilon}$ (Figure 8a of this paper). However, in that range of c, the theory does not describe the OFB *terminal* mode distribution (observed as ω dependence of the phase angle of complex mechano-optic coefficients; cf. Figure 11 of ref 33), again in harmony with the results for the dielectric mode distribution (cf. Figures 3 and 13 of this paper). For the dielectric mode distribution, the disagreements between the data and prediction are due to the considerably weak c dependence of the $\tau_{p,\epsilon}$ span (cf. Figure 8b) and the rather strong c dependence of the intensity distribution (Figure 12), both being not described by the theory. From this fact, one may speculate that the disagreements for the OFB mode distribution are also due to theoretically-unexpected, weak and strong c dependence of the $\tau_{p,\mathrm{OFB}}$ span and intensity ($g_{p,\mathrm{OFB}}$) distribution for slow OFB modes.

However, we should also note an important difference between dielectric and OFB/viscoelastic relaxation. The dielectric relaxation of type-A chains detects orientational correlation at two separate times that is represented by the local correlation function, $C(n,t;m)$ (eq 1). On the other hand, both OFB and viscoelastic relaxation at long time scales reflect decay of orientational anisotropy with time that is described by an orientation function,[10,15,25]

$$S(n,t) = \langle \mathbf{u}(n,t)\, \mathbf{u}(n,t) \rangle_{xy} \qquad (20)$$

As explained in our previous paper,[15] $C(n,t;m)$ and $S(n,t)$ represent different averages (first- and second-order moment) of the bond vector $\mathbf{u}(n,t)$ at time t so that a relationship between C and S is dependent on the nature of chain dynamics: For an extreme case of incoherent chain motion, $S(n,t)$ after a step-strain at $t = 0$ is expanded with respect to f_p and $\tau_{p,\epsilon}$ for C (eq 2) as[15]

$$S(n,t) = S_0 \frac{2}{N} \sum_{p=1}^{N} [f_p(n)]^2 \exp(-2t/\tau_{p,\epsilon}) \qquad (21)$$

with S_0 being a constant. For this case, $\tau_{p,\mathrm{OFB}}$ and $g_{p,\mathrm{OFB}}$ of the pth viscoelastic/OFB mode are given by $\tau_{p,\epsilon}/2$ and an integral, $(2/N)\int_0^N f_p^{\,2}\, dn$, respectively. On the other hand, for the other extreme case of highly coherent motion, we find[15]

$$S(n,t) = S_0 \frac{2}{N} \sum_{p=1}^{N} [\int_0^N f_p(m)\, dm]\, f_p(n) \exp(-t/\tau_{p,\epsilon}) \qquad (22)$$

For this case, we have $\tau_{p,\mathrm{OFB}} = \tau_{p,\epsilon}$ and $g_{p,\mathrm{OFB}} \propto (2/N)[\int_0^N f_p\, dn]^2$. As noted from the difference between these two cases, the c dependence of $\tau_{p,\mathrm{OFB}}$ and $g_{p,\mathrm{OFB}}$ for the viscoelastic/OFB modes would be qualitatively similar but not necessarily identical to the dependence of the dielectric $\tau_{p,\epsilon}$ and $g_{p,\epsilon}$. From this point of view, it is very interesting to experimentally compare dielectric and viscoelastic/OFB behavior of the PI/OB-0.7 solutions used in this paper. An attempt is now being made, and the results will be presented in our future paper.

V-4. Origin of Changes in Eigenmodes. As concluded in section V-2, the broadening of the ϵ'' curves with c_{PI} essentially reflects deviation of F_p from the sinusoidal F_p° of various models (eq 10). Previous discussion considering analogies between the eigenfunction equation and the Schrödinger equation suggests that differences between F_p and F_p° (Figure 10) are attributed to some extra relaxation source at chain ends that is not considered in the models.[14] There are various mechanisms that could, in principle, provide this source to broaden the ϵ'' curves.

The PI chains examined in this paper are entangled at $c_{\mathrm{PI}} > 0.272$ g cm^{-3} (cf. Figure 1), and the broadening of the ϵ'' curves completes in this range of c_{PI} (cf. Figures 3 and 4). From this fact, one might tend to attribute the changes of F_p and broadening of ϵ'' curves to the entanglement mechanism. However, we have already demonstrated that entangled and unentangled, bulk regular PI chains exhibit indistinguishable, broad shapes of the ϵ'' curves.[15] This fact indicates that the broadening of the ϵ'' curves is *not* due to the entanglement mechanism defined in the usual sense as the mechanism leading to the 3.5th power law behavior of τ_1 and viscosity of linear chains.

Since changes of F_p and ϵ'' curves are observed for $c_{\mathrm{PI}} > c^*$, the chain overlapping should be essential for those changes. We may speculate that the motion of a chain is coupled with motion of overlapping chains at $c_{\mathrm{PI}} > c^*$ and pure Rouse/Zimm eigenmodes of each chain are mixed into new eigenmodes having nonsinusoidal F_p. From this point of view, the Fourier expansion coefficients a_{pi} (Figure 11) can be used as a measure for the extent of mixing for the Rouse/Zimm modes. However, details in the coupling of chain motion are not yet understood. It is also unclear how the coupling effectively enhances relaxation at chain ends (as compared to the chain center) to provide nonsinusoidal nature to F_p (Figure 10) without affecting much of the τ_p span (Figures 7 and 8). Further studies are necessary for the changes of F_p and τ_p spans with c_{PI}.

VI. Concluding Remarks

We have examined the dielectric behavior for solutions of dipole-inverted PI chains. Eigenmode analyses

indicated that the (integrated) eigenfunctions F_p become nonsinusoidal with increasing $c_{PI} > c^*$ while the span of relaxation times τ_p is only weakly dependent on c_{PI}. Thus, the observed broadening of the ϵ'' curves with c_{PI} is essentially due to changes in F_p, not due to the changes in the τ_p span. This experimental fact rules out previous arguments for the dielectric mode distribution and τ_1 that were based on the scheme of changes in the τ_p span. The changes in F_p may be attributed to coupling of motion of overlapping chains that could induce mixing of pure Rouse/Zimm modes into new eigenmodes having nonsinusoidal F_p. However, details of the coupling mechanism are not specified yet. The changes of F_p and τ_p spans with c_{PI} deserve further attention.

Acknowledgment. We thank Dr. A. Kajiwara and Prof. M. Kamachi at Osaka University for their help for oligo-GPC measurements. We thank Prof. K. Osaki at Kyoto University and Prof. T. Lodge at University of Minnesota for their valuable and stimulating comments on this work. We acknowledge with thanks the financial support for this study from Ministry of Education, Science and Culture, Japan, under the Grant No. 06651054.

References and Notes

(1) Stockmayer, W. H. *Pure Appl. Chem.* **1967**, *15*, 539.
(2) (a) Baur, M. E.; Stockmayer, W. H. *J. Chem. Phys.* **1965**, *43*, 4319. (b) Stockmayer, W. H.; Burke, J. J. *Macromolecules* **1969**, *2*, 647.
(3) Imanishi, Y.; Adachi, K.; Kotaka, T. *J. Chem. Phys.* **1988**, *89*, 7585; see the references therein for the earlier work on polydisperse PI chains.
(4) Yoshida, H.; Adachi, K.; Watanabe, H.; Kotaka, T. *Polym. J. (Jpn.)* **1989**, *21*, 863.
(5) Adachi, K.; Yoshida, H.; Fukui, F.; Kotaka, T. *Macromolecules* **1990**, *23*, 3138.
(6) Yoshida, H.; Watanabe, H.; Adachi, K.; Kotaka, T. *Macromolecules* **1991**, *24*, 2981.
(7) Adachi, K.; Kotaka, T. *Prog. Polym. Sci.* **1993**, *18*, 585 and references therein.
(8) Boese, D.; Kremer, F.; Fetters, L. J. *Macromolecules* **1990**, *23*, 829; **1990**, *23*, 1826.
(9) (a) Watanabe, H.; Yamazaki, M.; Yoshida, H.; Adachi, K.; Kotaka, T. *Macromolecules* **1991**, *24*, 5365. (b) Watanabe, H.; Yamazaki, M.; Yoshida, H.; Kotaka, T. *Macromolecules* **1991**, *24*, 5372.
(10) Watanabe, H.; Kotaka, T. *CHEMTRACTS: Macromol. Chem.* **1991**, *2*, 139 and references therein.
(11) Patel, S. S.; Takahashi, K. M. *Macromolecules* **1992**, *25*, 4382.
(12) Urakawa, O.; Adachi, K.; Kotaka, T. *Macromolecules* **1993**, *26*, 2036.
(13) Urakawa, O.; Adachi, K.; Kotaka, T. *Macromolecules* **1993**, *26*, 2042.
(14) Watanabe, H.; Urakawa, O.; Kotaka, T. *Macromolecules* **1993**, *26*, 5073.
(15) Watanabe, H.; Urakawa, O.; Kotaka, T. *Macromolecules* **1994**, *27*, 3525.
(16) Urakawa, O.; Adachi, K.; Kotaka, T.; Takemoto, Y.; Yasuda, H. *Macromolecules* **1994**, *27*, 7410.
(17) Muthukumar, M.; Freed, K. F. *Macromolecules* **1978**, *11*, 843.
(18) Muthukumar, M. *Macromolecules* **1984**, *17*, 971.
(19) The dipole-inverted PI chains ($M_{PI} \simeq 48$K) used in this study are subjected to an excluded-volume interaction, while eqs 6–8 are obtained on the basis of a relationship valid for Gaussian chains, $\langle \Delta R^2 \rangle = N\langle u^2 \rangle$. However, for those PI chains the expansion factor is small ($\alpha = 1.12$) and the excluded-volume interaction is not significant. Thus, we may use eqs 6–8 as a good approximation for the PI chains in OB-0.7.
(20) These M_c values for solutions were evaluated as $M_c = M_c^{bulk}/\phi_{PI}$, with $M_c^{bulk} = 10$K (for bulk PI)[21] and ϕ_{PI} = PI volume fraction in the solutions.
(21) See, for example: Graessley, W. W. *Adv. Polym. Sci.* **1974**, *16*, 38.
(22) Tsunashima, Y.; Hirata, N.; Nemoto, N.; Kurata, M. *Macromolecules* **1988**, *21*, 1107.
(23) Urakawa, O. Ph.D. Thesis, Osaka University, 1994.
(24) See, for example: Yamakawa, H. *Modern Theory of Polymer Solutions*; Harper & Row: New York, 1971; Chapter 6.
(25) See, for example: Doi, M.; Edwards, S. F. *The Theory of Polymer Dynamics*; Clarendon: Oxford, 1986; Chapters 6 and 7.
(26) Tschoegl, N. W. *J. Chem. Phys.* **1964**, *40*, 473.
(27) This ϵ value, 0.2, was chosen so that the observed τ_2/τ_1 ratio (=1/3.34) of the dilute PI chains was described by the Tschoegl model (cf. eq 13).
(28) Concerning the failure of the Rouse and Zimm models for explaining the dielectric behavior of dilute chains in good solvents, we have to reexamine the meaning of universal proportionality between τ_1 and $M\eta_s[\eta]/RT$ (η_s = solvent viscosity) reported by Adachi et al.[16] for dilute solutions of various type-A chains in various solvents (including both Θ and good solvents). An obvious point is that the M dependence of τ_1 and $[\eta]$ reflecting features of chain dynamics is *not* explicitly involved in the proportionality. We also note that various models predict different M dependence of τ_1 but still lead to the proportionality between τ_1 and $M[\eta]$ and that the $\tau_1/M\eta_s[\eta]$ ratio is insensitive to the model features. Thus, the proportionality (being universal within experimental uncertainties) does not specify the validity of a particular model. In fact τ_1's for dilute chains in Θ and good solvents, satisfying this experimentally universal proportionality, are to be explained from different models, e.g., Zimm and Tschoegl models.
(29) Johnson, R. M.; Schrag, J. L.; Ferry, J. D. *Polym. J.* **1970**, *1*, 742.
(30) Ferry, J. D. *Viscoelastic Properties of Polymers*, 3rd ed.; Wiley: New York, 1980; Chapter 9.
(31) Lodge, T. P.; Miller, J. M.; Schrag, J. L. *J. Polym. Sci., Polym. Phys. Ed.* **1982**, *20*, 1409.
(32) Lodge, T. P.; Schrag, J. L. *Macromolecules* **1892**, *15*, 1376; **1984**, *17*, 352.
(33) Martel, C. J. T.; Lodge, T. P.; Dibbs, M. G.; Stokich, T. M.; Sammler, R. L.; Carriere, C. J.; Schrag, J. L. *Faraday Symp. Chem. Soc.* **1983**, *18*, 173.

MA9504734